

Supporting Information

Kotula et al. 10.1073/pnas.1321321111

SI Methods

To determine the ratio of *Escherichia coli* in the cI and Cro states in a population, we titered the *E. coli* to yield at least 100 single colonies on lactose indicator plates, and also plated at a 100-fold lower dilution, yielding at least 10,000 colonies.

On the latter plates colonies could not be counted but it was possible to recognize rare colonies of a distinct phenotype. Thus, in Figs. 2–4 and Fig. S6, where it is stated that 100% or 0% of cells have a certain phenotype, the limit of detection is about $1/10^4$.

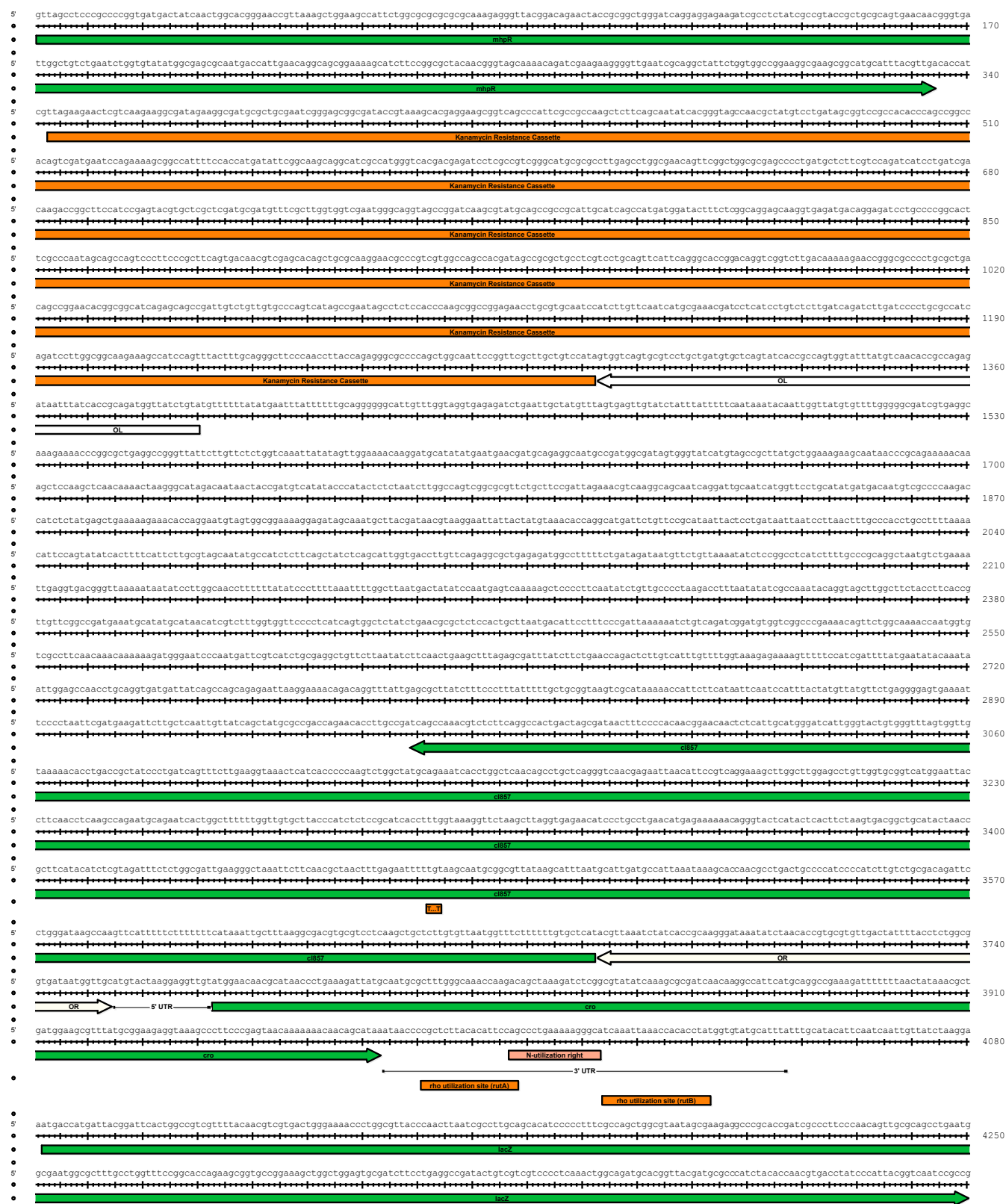


Fig. S1. Memory element in PAS129.

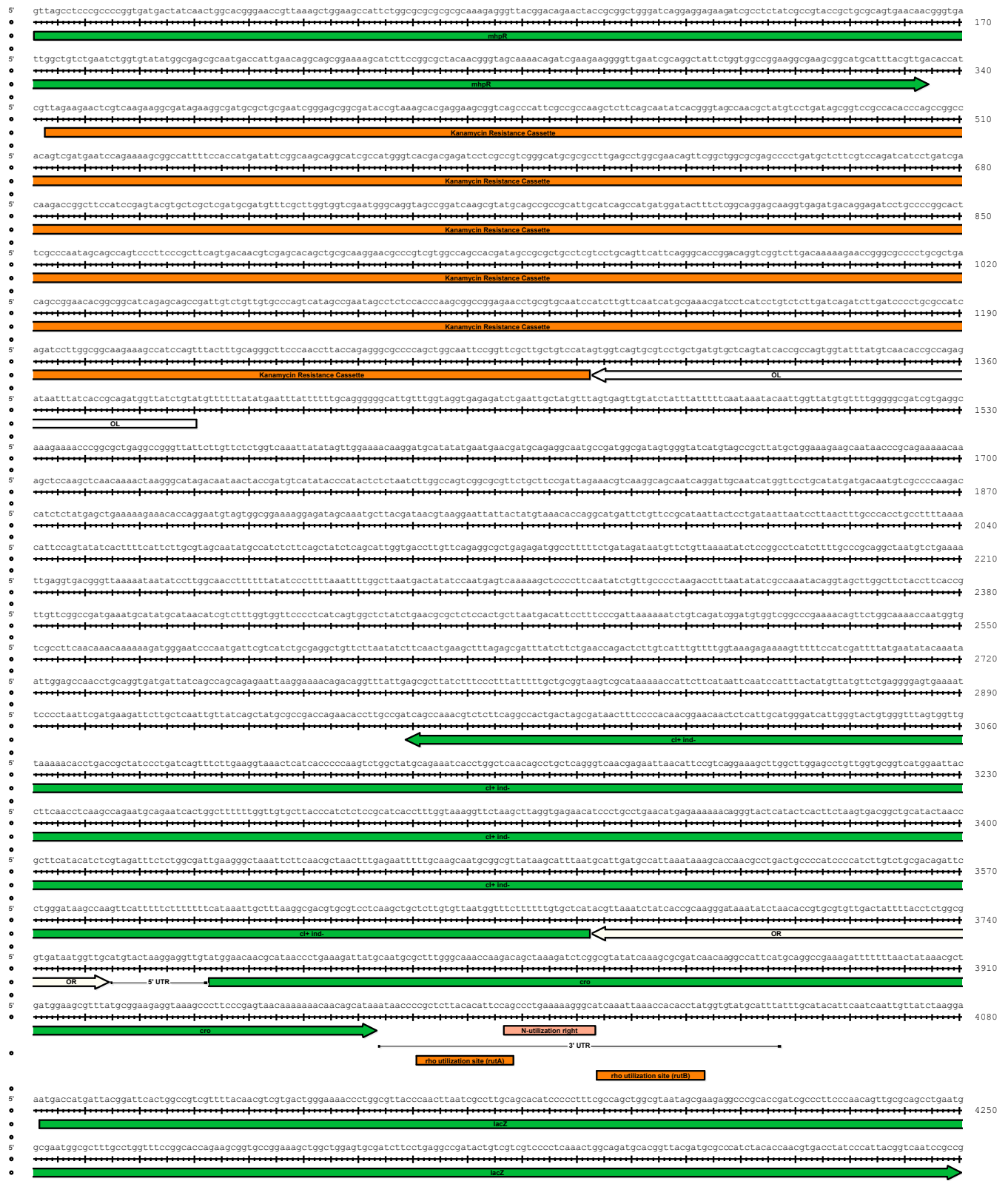


Fig. S2. Memory element in PAS130.

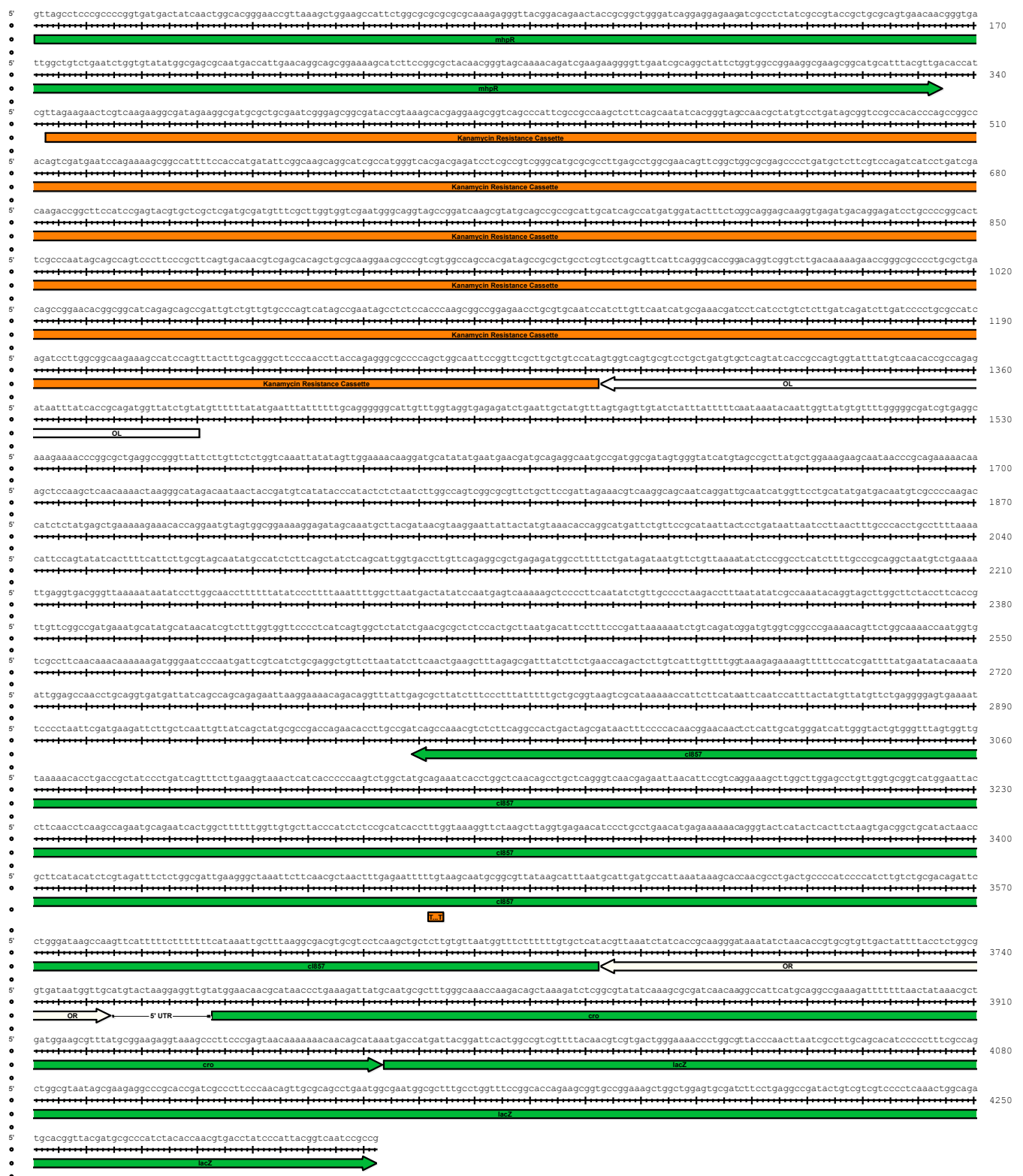


Fig. S3. Memory element in PAS131.

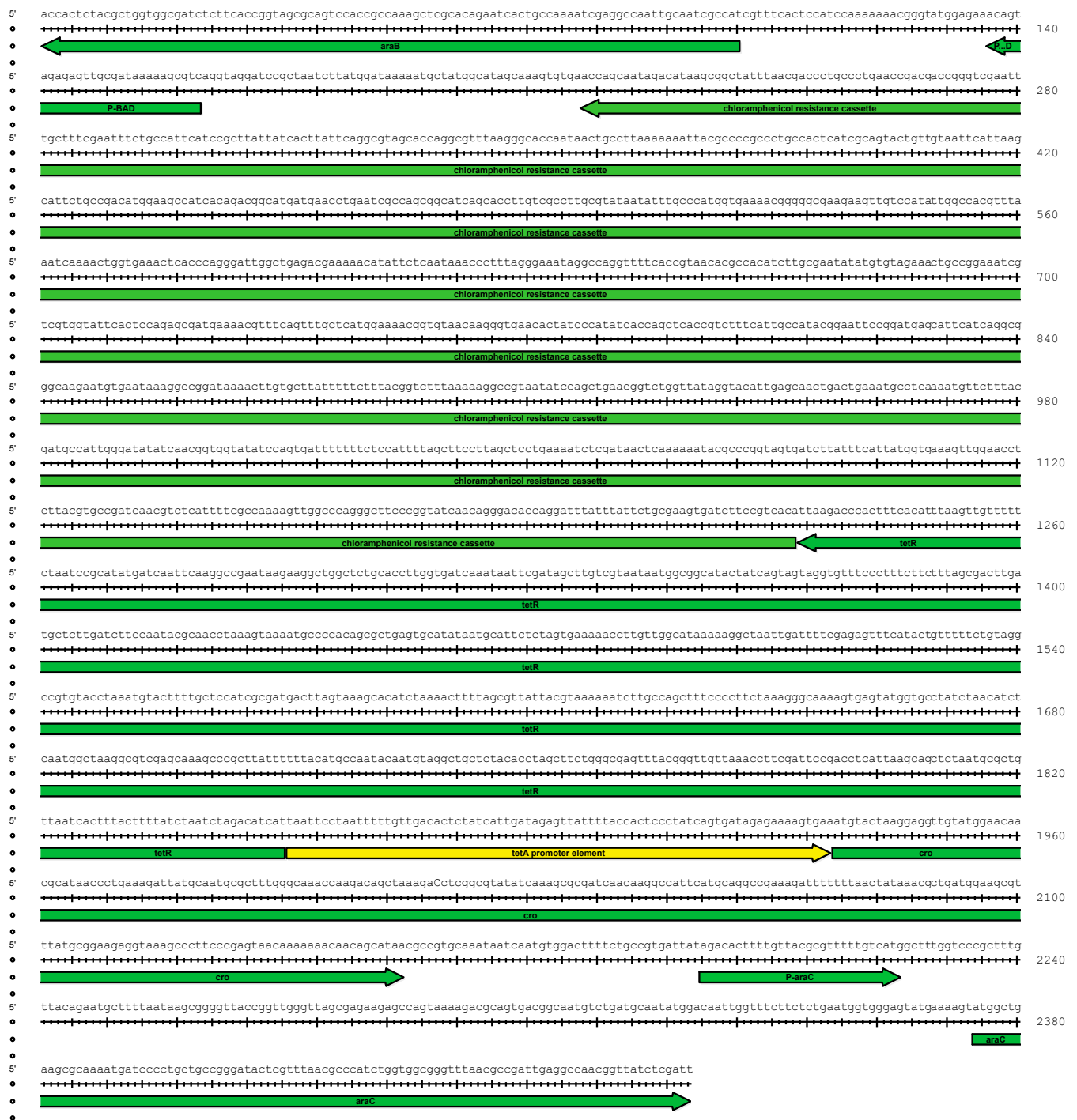


Fig. S5. The *tetP-cro* trigger element used in this study.

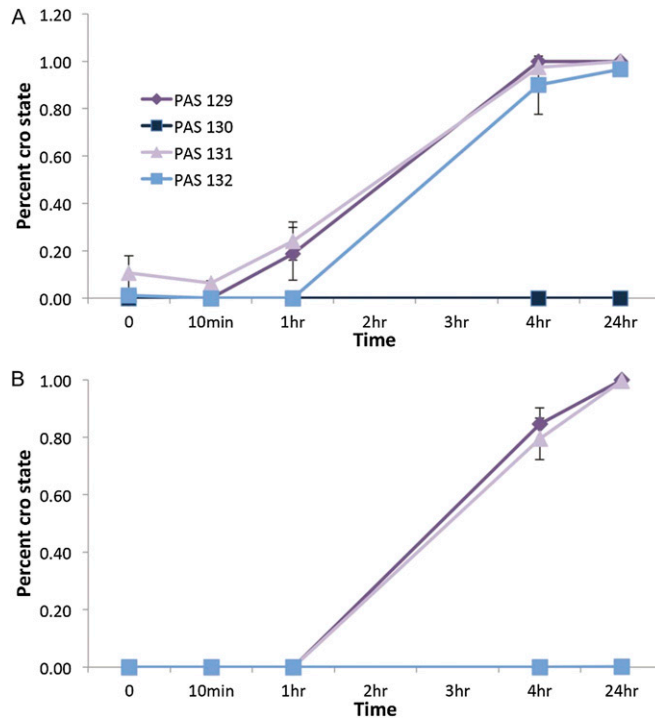


Fig. S6. Identification of a memory element with optimal switching properties. (A) Memory elements 11–14, which were integrated into strains PAS129-PAS132, were evaluated for switching in response to anhydrotetracycline (ATC). (B) PAS129-PAS132 were evaluated for switching in response to an incubation temperature of 42 °C, without ATC. For both panels, points represent the means \pm SD of three or more independent samples.

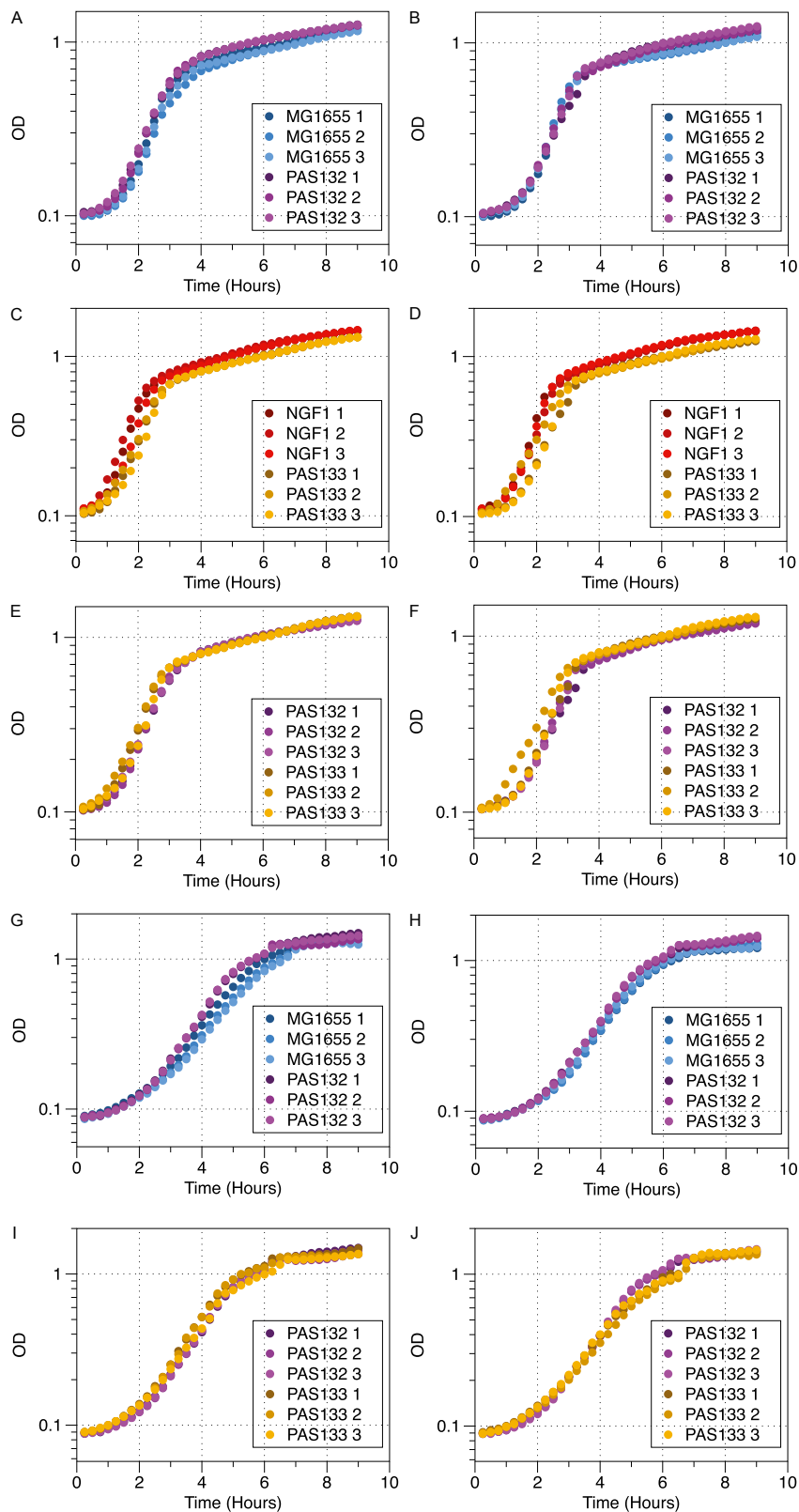


Fig. S7. Growth curves of engineered strains in brain-heart infusion (BHI) media. (A) Growth of MG1655 and PAS132 in BHI media without ATC. (B) Growth of MG1655 and PAS132 in BHI media with ATC. (C) Growth of NGF1 and PAS133 in BHI media without ATC. (D) Growth of NGF1 and PAS133 in BHI media with ATC. (E) Growth of PAS132 and PAS133 in BHI media without ATC. (F) Growth of PAS132 and PAS133 in BHI media with ATC. (G) Growth of MG1655 and PAS132 in M9 glucose + casamino acids media without ATC. (H) Growth of MG1655 and PAS132 in M9 glucose + casamino acids media with ATC. (I) Growth of PAS132 and PAS133 in M9 glucose + casamino acids media without ATC. (J) Growth of PAS132 and PAS133 in M9 glucose + casamino acids media with ATC.

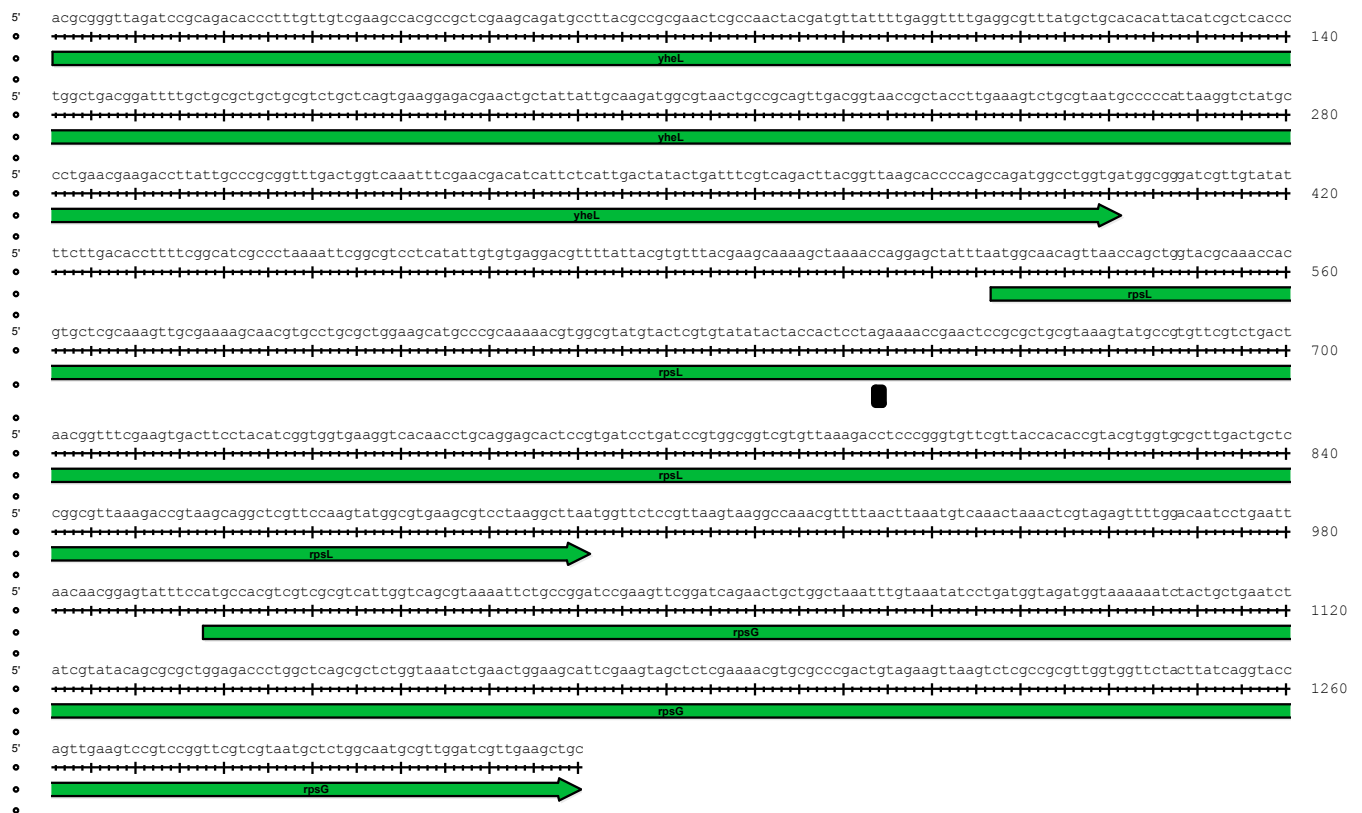


Fig. S8. Sequence of the *rpsL* mutation. The *rpsL* gene of PAS132 and MG1655 was amplified using 5'-CCA GCC AGA TGG CCT GG-3' and 5'-GAC GCG ACG ACG TGG C-3' primers, then sequenced. The sequences were compared using Lasergene software to identify the A430G mutation that resulted in a *Lys42Arg* mutation.

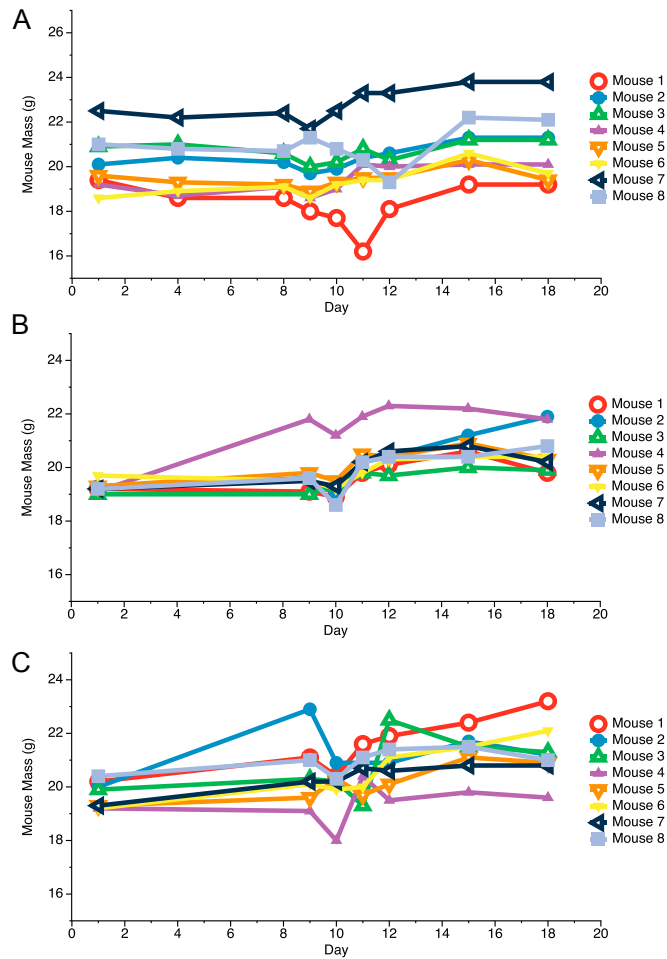


Fig. S9. Monitoring mouse weights. Mice were weighed on the indicated days to monitor their health. A drop in total body mass >20% would indicate that there was a potential health concern. From day 1 to day 18 of all in vivo experiments, all of the mice showed a net gain in total body mass. This gain indicated that administering two drugs, streptomycin and ATC, as well as our engineered bacteria, did not adversely affect mouse health. (A) In vivo experiment #1 corresponds to data presented in Fig. 3B. (B) In vivo experiment #2 corresponds to data presented in Fig. 3D. (C) In vivo experiment #3 corresponds to data presented in Fig. 4. Points represent the mass of an individual mouse on the specified day.

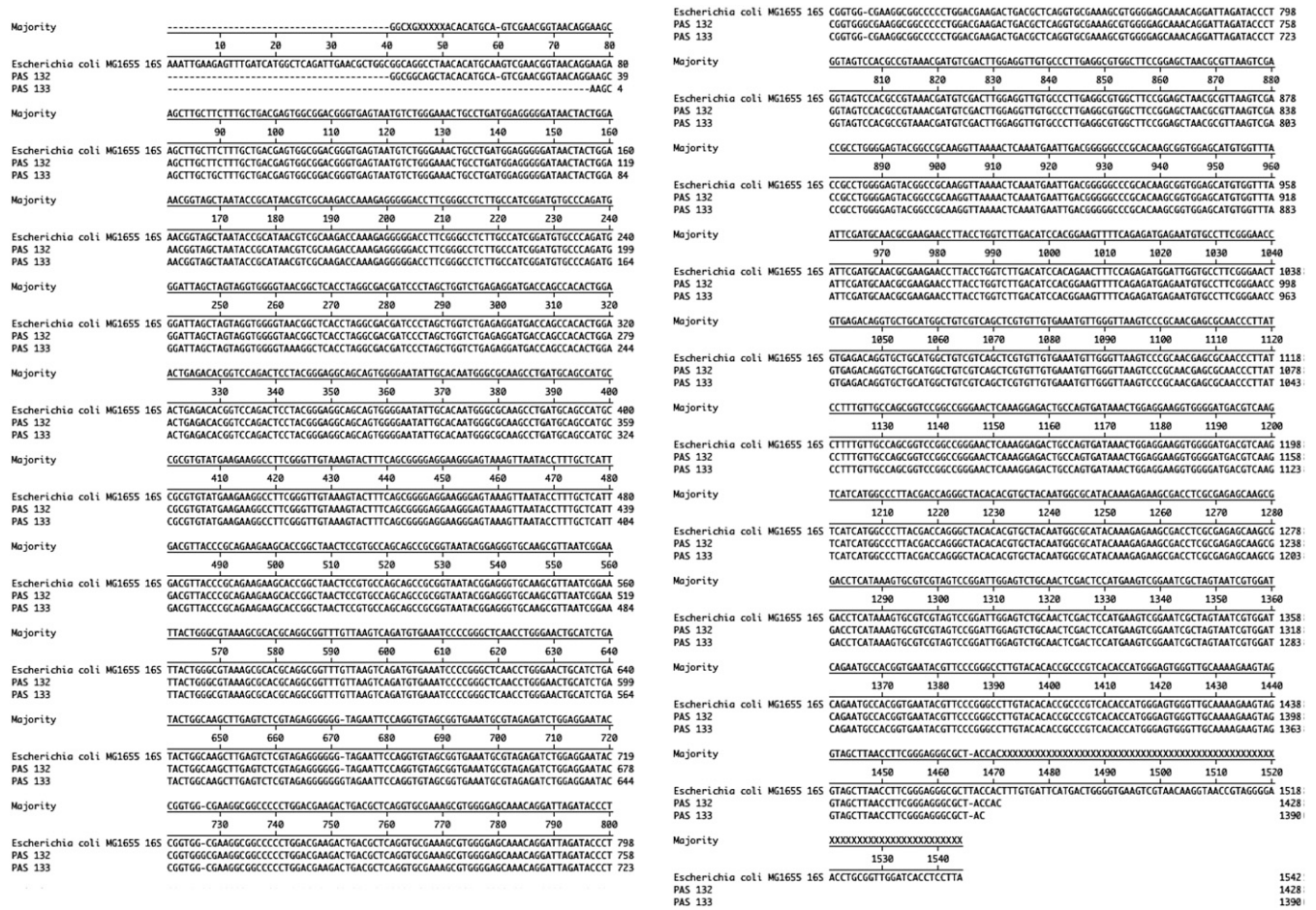


Fig. S10. Alignment of the 16S subunit of PAS132 and PAS133 with MG1655. The gene encoding the 16S ribosomal subunits of PAS132 and PAS133 were amplified by PCR, then sequenced (1). The sequences were aligned against the reference sequence of MG1655 using Lasergene software. A phylogenetic tree was constructed comparing the reference sequences of the indicated bacteria using Lasergene software.

1. Weisburg WG, Barns SM, Pelletier DA, Lane DJ (1991) 16S ribosomal DNA amplification for phylogenetic study. *J Bacteriol* 173(2):697-703.